

# Accepted Manuscript

## Design, Synthesis and Biological Evaluation of Novel Donepezil-Coumarin Hybrids as Multi-Target Agents for the Treatment of Alzheimer's Disease

Sai-Sai Xie, Jin-Shuai Lan, Xiaobing Wang, Zhi-Min Wang, Neng Jiang, Fan Li, Jia-Jia Wu, Jin Wang, Ling-Yi Kong

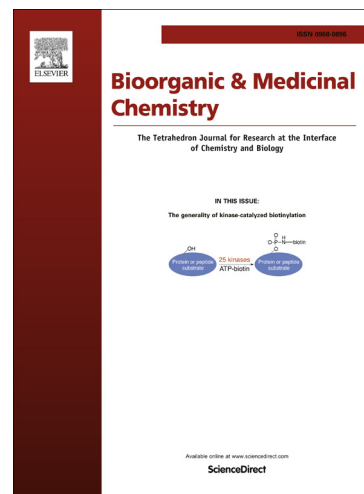
PII: S0968-0896(16)30103-1  
DOI: <http://dx.doi.org/10.1016/j.bmc.2016.02.023>  
Reference: BMC 12825

To appear in: *Bioorganic & Medicinal Chemistry*

Received Date: 6 November 2015  
Revised Date: 17 February 2016  
Accepted Date: 18 February 2016

Please cite this article as: Xie, S-S., Lan, J-S., Wang, X., Wang, Z-M., Jiang, N., Li, F., Wu, J-J., Wang, J., Kong, L-Y., Design, Synthesis and Biological Evaluation of Novel Donepezil-Coumarin Hybrids as Multi-Target Agents for the Treatment of Alzheimer's Disease, *Bioorganic & Medicinal Chemistry* (2016), doi: <http://dx.doi.org/10.1016/j.bmc.2016.02.023>

This is a PDF file of an unedited manuscript that has been accepted for publication. As a service to our customers we are providing this early version of the manuscript. The manuscript will undergo copyediting, typesetting, and review of the resulting proof before it is published in its final form. Please note that during the production process errors may be discovered which could affect the content, and all legal disclaimers that apply to the journal pertain.



**Design, Synthesis and Biological Evaluation of Novel Donepezil-Coumarin Hybrids as Multi-Target Agents for the Treatment of Alzheimer's Disease**

Sai-Sai Xie,<sup>†</sup> Jin-Shuai Lan,<sup>†</sup> Xiaobing Wang, Zhi-Min Wang, Neng Jiang, Fan Li, Jia-Jia Wu, Jin Wang, Ling-Yi Kong \*

*State Key Laboratory of Natural Medicines, Department of Natural Medicinal Chemistry, China Pharmaceutical University, 24 Tong Jia Xiang, Nanjing 210009, People's Republic of China*

\* Corresponding Author. Tel/Fax: +86-25-83271405; E-mail: cpu\_lykong@126.com;

<sup>†</sup>These authors contributed equally to this work.

**Abstract**

Combining *N*-benzylpiperidine moiety of donepezil and coumarin into in a single molecule, novel hybrids with ChE and MAO-B inhibitory activity were designed and synthesized. The biological screening results indicated that most of compounds displayed potent inhibitory activity for AChE and BuChE, and clearly selective inhibition to MAO-B. Of these compounds, **5m** was the most potent inhibitor for eeAChE and eqBuChE (0.87  $\mu$ M and 0.93  $\mu$ M, respectively), and it was also a good and balanced inhibitor to hChEs and hMAO-B (1.37  $\mu$ M for hAChE; 1.98  $\mu$ M for hBuChE; 2.62  $\mu$ M for hMAO-B). Molecular modeling and kinetic studies revealed that **5m** was a mixed-type inhibitor, which bond simultaneously to CAS, PAS and mid-gorge site of AChE, and it was also a competitive inhibitor, which occupied the active site of MAO-B. In addition, **5m** showed good ability to cross the BBB and had no toxicity on SH-SY5Y neuroblastoma cells. Collectively, all these results suggested that **5m** might be a promising multi-target lead candidate worthy of further pursuit.

**Keywords:** Alzheimer's disease, coumarin, donepezil, cholinesterase, monoamine oxidase, docking.

## 1. Introduction

Alzheimer's disease (AD) is the most common type of dementia clinically characterized by progressive loss of memory and deficits in different cognitive domains [1, 2]. It has been estimated that there were 36 million people with dementia in 2010, and this number will rise to 42.3 million in 2020 and 81.1 million by 2040 [3, 4]. Although several factors including low levels of acetylcholine (ACh), the formation of  $\beta$ -amyloid deposits, oxidative stress and dyshomeostasis of biometals have been demonstrated to play significant roles in the pathogenesis of AD, the exact etiology is still not fully understood [5, 6].

The current strategies for AD treatment are mainly based on cholinergic hypothesis, which suggests that a decline of ACh levels in specific brain regions leads to cognitive and memory deficits, and sustaining or recovering cholinergic function can alleviate these symptoms [7, 8]. Supporting this notion that four cholinesterase inhibitors (ChEIs), tacrine, rivastigmine, galanthamine and donepezil, have been approved in clinical use [9]. However, due to the complex nature of AD, these drugs can only reverse the symptoms for a short period of time instead of halting or curing the neurodegeneration [10]. Thus, a more appropriate approach termed the Multi-Target Directed Ligands (MTDLs) strategy has been proposed to face this disease [11-13]. MTDLs mean a single compound that can simultaneously modulate different targets involved in the neurodegenerative AD cascade [14, 15]. One of the most widely adopted approaches for designing MTDLs is to modify a ChEI and render it exert other biological properties useful for treating AD[16].

MAOs are flavin adenine dinucleotide (FAD)-containing enzymes responsible for the oxidative deamination of endogenous monoamine neurotransmitters, trace amines, and a number of amine xenobiotics [17, 18]. Two isoforms, namely MAO-A and -B, have been identified based on substrate selectivity and inhibitor sensitivity [19]. MAO-A preferentially deaminates serotonin, adrenaline and noradrenaline, and is selectively and irreversibly inhibited by clorgyline, while MAO-B preferentially deaminates  $\beta$ -phenylethylamine and benzylamine, and is irreversibly inhibited by R-(-)-deprenyl [20, 21]. It was found that MAO-B activity increases with age. Especially in AD, a significant rise in MAO-B activity was found in cerebral spinal fluid (CSF), brain tissue as well as in platelets [22, 23]. The high levels of MAO-B in neuronal tissue could lead to an increase in the level of  $H_2O_2$  and oxidative free radicals, which ultimately contribute to the etiology of AD [24]. Thus, selective inhibition of MAO-B becomes another valuable approach for the treatment of AD.

In recent years, many MTDLs have been designed and synthesized by combining the ChEI and MAO-B inhibitor into one molecule [25-33]. Because studies suggest that simultaneous inhibition of MAO-B and ChE can not only improve the level of ACh and reduce oxidative stress in brain but also can decrease  $\beta$ -amyloid deposition, another hallmark in AD pathogenesis, which will be more effective against AD [34]. Among all these MTDLs, TV2236 (Ladostigil) has been approved for phase IIb clinical trial, which prompt us to search new multi-target compounds with ChE and MAO-B inhibitory activity.

Very recently, we have reported a series of tacrine-coumarin hybrids as

multi-target compounds for treatment of AD (Figure 1) [35]. The tacrine was used to inhibit ChEs, and the coumarin moiety was chosen to inhibit MAOs. Among these compounds, compound **1** displayed potent inhibitory activity toward AChE and BuChE, and clearly selective inhibition for MAO-B. However, due to the presence of tacrine moiety [36], this compound showed severe hepatotoxicity (unpublished work), which hindered its further application.

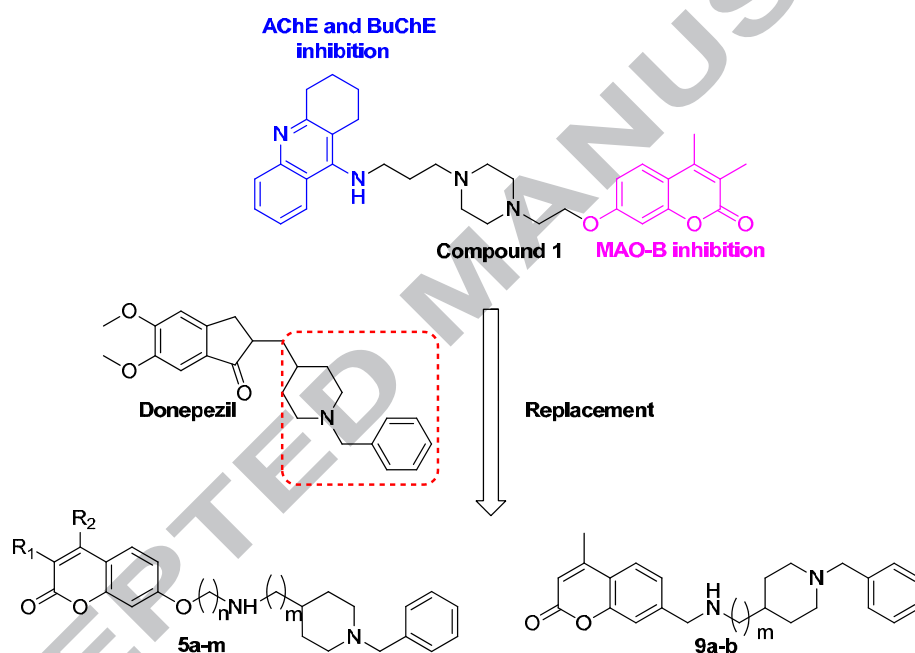


**Figure 1.** Design strategy for donepezil-coumarin hybrids.

In order to continue our work to discovery new multi-target compounds with both ChE and MAO-B inhibitory activity and to optimize the tacrine-coumarin hybrids, in this study, we wanted to replace the tacrine with a *N*-benzylpiperidine moiety based on donepezil to design a series of novel donepezil-coumarin hybrids as multi-target compounds for the treatment of AD. Compared to tacrine, donepezil was

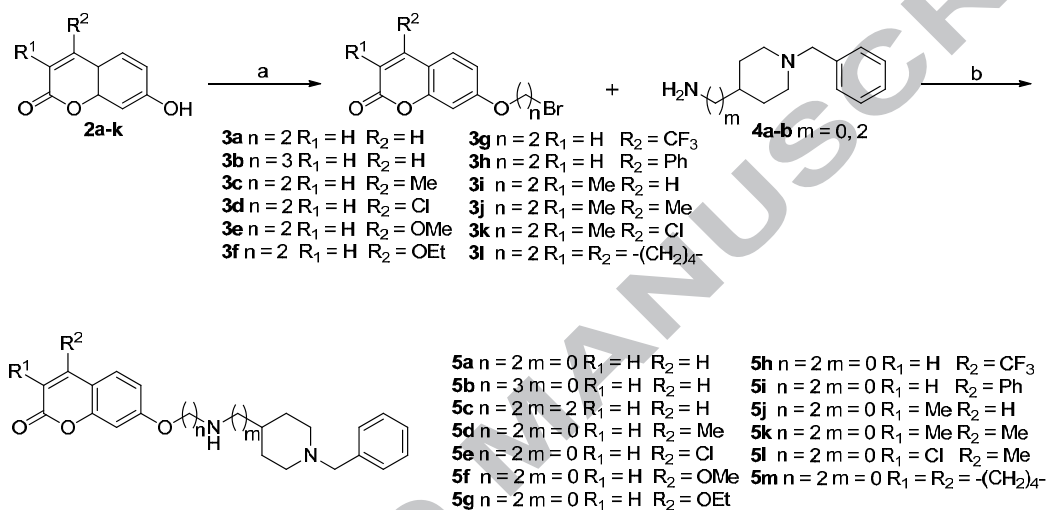
more potent and had no hepatotoxicity [37, 38]. The *N*-benzylpiperidine moiety, like tacrine, could inhibit the ChEs through binding to the catalytic anionic site (CAS) of ChEs. The design strategy of new compounds is shown in Figure 1. Similar to our previous design, the flexible alkyl chain was retained to connect coumarin and *N*-benzylpiperidine moiety, because such linker could be lodged by the AChE cavity, allowing the hybrids simultaneously to interact with PAS and CAS of the enzyme [39, 40]. Meanwhile, the position of the linker tethered to coumarin was unchanged in order to better evaluate the effect of this replacement design. In addition, to find the optimal length for ChE inhibition, the linker length was varied in initial step. Once the optimal length was obtained, different substituents were introduced to 3- and/or 4-position of coumarin ring to investigate the possible effects on both ChE and MAO inhibition. All designed compounds were synthesized and evaluated for their ability to inhibit ChEs and MAOs. The kinetic and molecular modeling studies were carried out to investigate interaction mechanism of selected compounds with AChE and MAO-B. The blood-brain barrier (BBB) permeation and the in vitro SH-SY5Y neuroblastoma cell toxicity assays were also performed to test the preliminary drug-like properties of selected compounds. Herein, we report the design, synthesis and evaluation of a series of novel donepezil-coumarin hybrids as multi-target compounds for AD treatment.

## 2. Result and Discussion

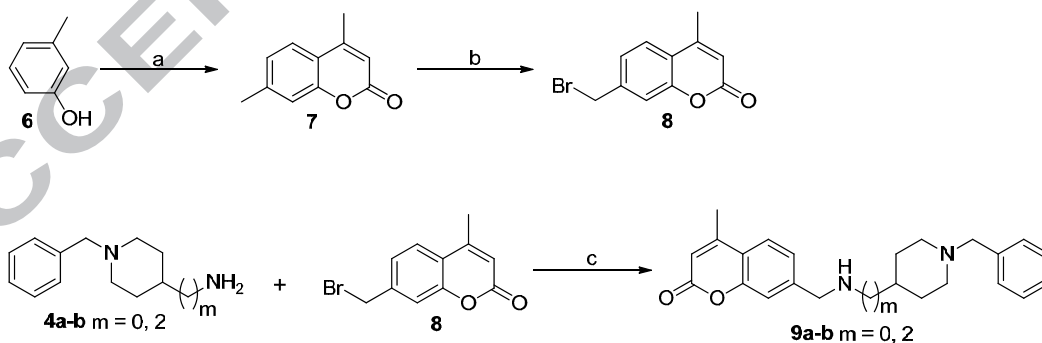
### 2.1 Chemistry

The synthesis of the designed compounds **5a-m** is illustrated in Scheme 1. The coumarin derivatives **2a-k** were obtained according to the previous reported methods

[28, 29, 35, 41-43]. Reacting the compounds **2a-k** with the corresponding  $\alpha$ ,  $\omega$ -dibromoalkanes afforded the key intermediates **3a-l**, which was then treated with commercially available compounds **4a-b** in the presence of potassium carbonate in acetonitrile to give the target compounds **5a-m**.



**Scheme 1.** Synthesis of compounds **5a-m**. Reagents and conditions: (a)  $Br(CH_2)_nBr$ , anhydrous  $K_2CO_3$ , acetone, reflux, 4 h; (b) Anhydrous  $K_2CO_3$ ,  $CH_3CN$ , reflux, 8 h.



**Scheme 2.** Synthesis of compounds **9a-b**. (a) Ethyl acetoacetate, conc.  $H_2SO_4$  (cat.), 1,4-dioxane,  $60^\circ C$ , 4 h; (b) NBS, dry benzene, benzoyl peroxide, reflux., 16 h. (c) Anhydrous  $K_2CO_3$ ,  $CH_3CN$ , reflux, 8 h.

For compounds **9a-b**, they were easily synthesized by the route shown in Scheme 2. Condensation of *m*-cresol with ethyl acetoacetate in the presence of a catalytic amount of concentrated sulfuric acid in 1, 4-dioxane provided compound **7**. The obtained **7** was selectively brominated at the 7-methyl group by NBS in dry benzene to give compound **8** [44]. Finally, using same condition for preparation of compounds **5a-m**, compound **8** was reacted with **4a-b** to furnish the desired compounds **9a-b**.

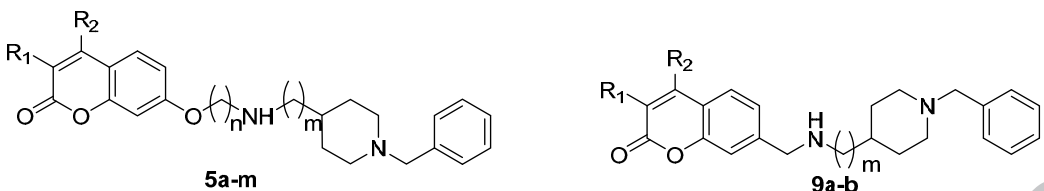
## 2.2 In Vitro Inhibition of ChEs

The inhibitory activities of the test compounds **5a-m** and **9a-b** against eeAChE (from electric eel) and eqBuChE (from equine serum) were determined according to the spectrophotometric method described by Ellman et al [45]. For comparison purpose, tacrine and donepezil were used as reference compounds. The IC<sub>50</sub> values of all test compounds and their selectivity index for eeAChE over eqBuChE are summarized in Table 1. From the table, it is interesting to note that, unlike donepezil which showed selectively inhibition for AChE (SI = 94.8), all compounds showed the balanced inhibition for both AChE and BuChE. Considering increasing attention to BuChE, these compounds might be more advantageous in AD treatment [46, 47].

The previous works demonstrated that the linker length connected the CAS and PAS binding moieties is critical for ChE inhibition [24, 29, 41, 48, 49]. Therefore, to get the optimal linker length, compounds **5a-c** with varying linker length between coumarin and *N*-benzyl piperidine moieties were synthesized in first step. The results



shown in Table 1 indicated compound **5a** showed the most potent inhibitory activity among these three compounds, which suggested that the short linker ( $n = 2$  and  $m = 0$ ) was more beneficial for ChE inhibition and thus selected as the optimal linker length. With the optimal length in hand, we next introduced different substituents to 3- and/or 4-position of coumarin moiety and investigated their possible effects on ChE inhibition. Unlike the previous reports [29, 41, 42], introduction of mono-substituent to 3- or 4-position of coumarin moiety did not remarkably influence the inhibitory activity in present study. Compounds **5d** and **5f-j** exhibited the inhibitory activity similar to their no substituted analogue **5a**. Only compound **5e** which have a chloro group ( $IC_{50} = 1.50 \mu\text{M}$  for eeAChE;  $IC_{50} = 1.48 \mu\text{M}$  for eqBuChE) on the 4-position of coumarin ring showed the activity higher than that of **5a** ( $IC_{50} = 4.42 \mu\text{M}$  for eeAChE;  $IC_{50} = 5.34 \mu\text{M}$  for eqBuChE). However, simultaneous substitution of 3- and 4-position at coumarin moiety afforded compounds **5k-m**, which could increase the activity in both ChE inhibition. Especially, 3,4-cyclohexane-fused coumarin **5m** showed the most potent inhibitory activity in this series with  $IC_{50}$  value of  $0.87 \mu\text{M}$  and  $0.93 \mu\text{M}$  against eeAChE and eqBuChE, respectively. In addition to the above investigation, the effects on ChE inhibition of replacement of oxygen atom linked to 7-position of coumarin moiety with carbon atom were also explored. The results indicated that compound **9b** having a two-carbon linker ( $m = 2$ ) between amino group and *N*-benzyl piperidine moiety was more potent inhibitor for both ChEs than compound **9a**.

**Table 1.** Inhibition of eeAChE and eqBuChE by Compounds **5a-m** and **9a-b**.


compd	R <sub>1</sub>	R <sub>2</sub>	n	m	IC <sub>50</sub> (μM)		SI <sup>c</sup>
					eeAChE <sup>a</sup>	eqBuChE <sup>b</sup>	
<b>5a</b>	H	H	2	0	4.42 ± 0.12	5.34 ± 0.45	1.21
<b>5b</b>	H	H	3	0	11.71 ± 0.92	9.86 ± 0.91	0.84
<b>5c</b>	H	H	2	2	8.91 ± 0.63	9.79 ± 0.16	1.10
<b>5d</b>	H	Me	2	0	5.62 ± 0.22	4.38 ± 0.42	0.78
<b>5e</b>	H	Cl	2	0	1.50 ± 0.27	1.48 ± 0.17	0.99
<b>5f</b>	H	OMe	2	0	6.29 ± 0.31	5.64 ± 0.55	0.90
<b>5g</b>	H	OEt	2	0	6.34 ± 0.25	6.95 ± 0.22	1.10
<b>5h</b>	H	CF <sub>3</sub>	2	0	9.18 ± 0.32	10.22 ± 1.07	1.11
<b>5i</b>	H	Ph	2	0	9.65 ± 0.45	8.93 ± 0.79	0.92
<b>5j</b>	Me	H	2	0	6.03 ± 0.59	7.53 ± 0.62	1.25
<b>5k</b>	Me	Me	2	0	1.48 ± 0.31	1.67 ± 0.18	1.13
<b>5l</b>	Cl	Me	2	0	1.58 ± 0.21	1.42 ± 0.29	0.90
<b>5m</b>	-(CH <sub>2</sub> ) <sub>4</sub> -		2	0	0.87 ± 0.09	0.93 ± 0.44	1.07
<b>9a</b>	H	Me	-	0	7.28 ± 0.61	10.83 ± 1.01	1.49
<b>9b</b>	H	Me	-	2	0.91 ± 0.17	0.96 ± 0.03	1.05
<b>donepezil</b>	-	-	-	-	0.04 ± 0.003	3.79 ± 0.01	94.8
<b>tacrine</b>	-	-	-	-	0.11 ± 0.01	0.02 ± 0.001	0.18

<sup>a</sup>The 50% inhibition at the indicated concentration (means ± SD of three experiments) of AChE from electric eel. <sup>b</sup>The 50% inhibition at the indicated concentration (means ± SD of three experiments) of BuChE from equine serum. <sup>c</sup>AChE selectivity index = IC<sub>50</sub>(eqBuChE)/IC<sub>50</sub>(eeAChE).

To further evaluate the inhibitory activity of the present compounds on ChEs, compounds **5e**, **5k-m** and **9b** with high inhibitory activity on ChEs of animal origin were selected to test on human ChEs. It can be seen from the Table 2 that compounds **5e** and **5k-l** exhibit the inhibitory activity for hChEs in the same range as that for animal ChEs. The inhibitory activity of compound **5m** for hChEs was little decreased in comparison to its inhibitory activity for animal ChEs. Interestingly, compound **9b** showed the most potent inhibition for hAChE in this series with IC<sub>50</sub> value of 0.067 μM, which was 13.6-fold more efficient for inhibition of eeAChE. However, its inhibitory activity for hBuChE was remarkably decreased (IC<sub>50</sub> = 0.96 μM for eqBuChE; IC<sub>50</sub> = 3.45 μM for hBuChE), and thus making it a clearly selective inhibitor for hAChE.

**Table 2.** Inhibition of hAChE and hBuChE by Compounds **5e**, **5k-m** and **9b**.

compd	IC <sub>50</sub> (μM)		SI <sup>c</sup>
	hAChE (μM) <sup>a</sup>	hBuChE (μM) <sup>b</sup>	
<b>5e</b>	2.04 ± 0.11	2.93 ± 0.15	1.43
<b>5k</b>	1.69 ± 0.09	2.67 ± 0.14	1.58
<b>5l</b>	1.82 ± 0.14	1.68 ± 0.13	0.92
<b>5m</b>	1.37 ± 0.05	1.98 ± 0.08	1.45
<b>9b</b>	0.067 ± 0.001	3.45 ± 0.76	51.49
<b>donepezil</b>	0.01 ± 0.002	2.74 ± 0.16	274

<sup>a</sup> The 50% inhibition at the indicated concentration (means ± SD of three experiments) of human AChE. <sup>b</sup> The 50% inhibition at the indicated concentration (means ± SD of three experiments) of human BuChE. <sup>c</sup> hAChE selectivity index = IC<sub>50</sub>(hBuChE)/IC<sub>50</sub>(hAChE).

### 2.3. In Vitro Inhibition of Human MAOs

To complete the multi-target biological profile of the target compounds, the inhibitory activity against hMAO-A and –B was measured, and a non-selective MAO inhibitor, iproniazide, was used as reference compound [50, 51]. As shown in Table 3, all compounds can effectively inhibit MAO-B at micromolar range, while no compound show significantly inhibitory activity for MAO-A at 100  $\mu\text{M}$ , indicating all compounds are clearly selective MAO-B inhibitors. Among these compounds, compound **9a** ( $\text{IC}_{50} = 1.93 \mu\text{M}$ ) showed the most potent inhibitor activity for MAO-B with  $\text{IC}_{50}$  value 4.1-fold more potent than that of iproniazide ( $\text{IC}_{50} = 7.97 \mu\text{M}$ ). However, different from our previous conclusion in tacrine-coumarin hybrids that substituents at 3- or/and 4-position of couamrin moiety could largely influence the inhibitory activity on MAOs [35], the present results did not give a clear structure-activity relationship (SAR). In view of all above results, compound **5m** presenting the most potent inhibition for animal ChEs and efficient inhibition for hChEs and hMAO-B was selected as promising compound for further study.

**Table 3** Inhibition of hMAO-A and hMOA-B by Compounds **5a-m** and **9a-b**.

compd	$\text{IC}_{50}$ ( $\mu\text{M}$ )		SI <sup>c</sup>
	hMAO-A <sup>a</sup>	hMAO-B <sup>b</sup>	
<b>5a</b>	N	$8.39 \pm 0.91$	$> 11.91$
<b>5b</b>	N	$12.6 \pm 1.2$	$> 7.94$
<b>5c</b>	N	$30.4 \pm 2.5$	$> 3.29$
<b>5d</b>	N	$2.75 \pm 0.22$	$> 36.36$
<b>5e</b>	N	$33.9 \pm 2.1$	$> 2.95$

<b>5f</b>	N	33.6 ± 0.9	> 2.98
<b>5g</b>	N	31.9 ± 1.9	> 3.13
<b>5h</b>	N	28.5 ± 1.7	> 3.51
<b>5i</b>	N	45.6 ± 3.6	> 2.19
<b>5j</b>	N	2.38 ± 0.11	> 42.01
<b>5k</b>	N	23.4 ± 1.1	> 4.27
<b>5l</b>	N	14.7 ± 1.5	> 6.80
<b>5m</b>	N	2.62 ± 0.81	> 38.17
<b>9a</b>	N	1.93 ± 0.33	> 51.81
<b>9b</b>	N	40.5 ± 4.1	> 2.47
<b>iproniazide</b>	6.57 ± 2.1	7.97 ± 1.5	0.82
<b>safinamide</b>	45.00 <sup>c</sup>	0.009 <sup>c</sup>	5000

<sup>a</sup>The 50% inhibition at the indicated concentration (means ± SD of three experiments) of human MAO-A. <sup>b</sup>The 50% inhibition at the indicated concentration (means ± SD of three experiments) of human MAO-B. <sup>c</sup>hMAO-B selectivity index = IC<sub>50</sub>(hMAO-A)/IC<sub>50</sub>(hMAO-B). N = no inhibitory activity was observed on MAO-A at 100 μM.<sup>c</sup> Values obtained from Ref. 52.

#### 2.4. Kinetic Study of ChE Inhibition

In order to investigate the inhibition mechanism of compound **5m**, an enzyme kinetic study was carried out. The type of inhibition was elucidated from the analysis of Lineweaver-Burk plots, which were reciprocal rates versus reciprocal substrate concentrations for the different inhibitor concentrations resulting from the substrate-velocity curves. For AChE, the plots (Figure 2) showed that both increasing slopes and intercepts at increasing inhibitor concentration. This pattern indicated a mixed-type inhibition and therefore revealed that compound **5m** might be able to bind to the catalytic active site (CAS) as well as peripheral anionic site (PAS) of AChE.

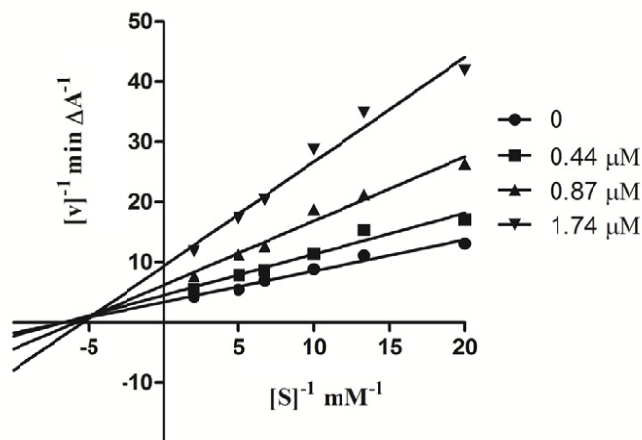


**Figure 2** Kinetic study on the mechanism of eeAChE inhibition by compound **5m**. Overlaid Lineweaver–Burk reciprocal plots of AChE initial velocity at increasing substrate concentration (0.05–0.50 mM) in the absence of inhibitor and in the presences of different concentrations of **5m** are shown.

In contrast, a different plot for BuChE was obtained (Figure 3), showing increasing slopes and constant intercepts in different inhibitor concentrations. This suggested a competitive inhibition, which revealed that compound **5m** might compete for the same binding site as the substrate acetylcholine.

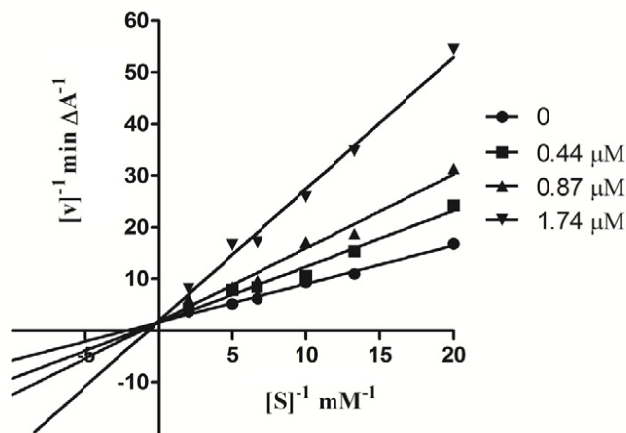


**Figure 3** Kinetic study on the mechanism of eqBuChE inhibition by compound **5m**. Overlaid

Lineweaver–Burk reciprocal plots of BuChE initial velocity at increasing substrate concentration (0.05–0.50 mM) in the absence of inhibitor and in the presences of different concentrations of **5m** are shown.

## 2.5. Reversibility and Kinetic Study of MAO-B Inhibition

From a therapeutic point of view, reversible inhibition of MAO-B may have significant advantages over the irreversible inactivation of the enzyme. Therefore, to investigate whether compound **5m** is a/an reversible or irreversible inhibitor of MAO-B, the recovery of enzymatic activity after dilution of the enzyme–inhibitor complexes was evaluated, and an irreversible inhibitor, pargyline, was used as reference compound [53]. MAO-B was pre-incubated with compounds **5m** at concentrations of 0, 10 and  $100 \times IC_{50}$  for 30 min and then diluted 100-fold to yield concentrations of 0, 0.1 and  $1 \times IC_{50}$ . For reversible inhibition, enzymatic activity is expected to recover to approximately 90% after dilution to  $0.1 \times IC_{50}$ , and 50% after dilution to  $1 \times IC_{50}$ . For an irreversible inhibitor, enzyme activity is expected not to recover after diluting the enzyme–inhibitor complex. From the Figure 4, it can be seen that, after the dilution of **5m** to  $0.1 \times IC_{50}$ , the MAO-B catalytic activities are recovered to levels of 86% of the control value (recorded in absence of inhibitor). After dilution to  $1 \times IC_{50}$ , the MAO-B catalytic activities are recovered to levels of 47%. This behavior is consistent with a reversible interaction of the compound with MAO-B. After similar incubation of MAO-B with the irreversible inhibitor pargyline at  $10 \times IC_{50}$ , and dilution of the enzyme–inhibitor complex to  $0.1 \times IC_{50}$ , the MAO-B

activities were not fully recovered (less than 10% of control).

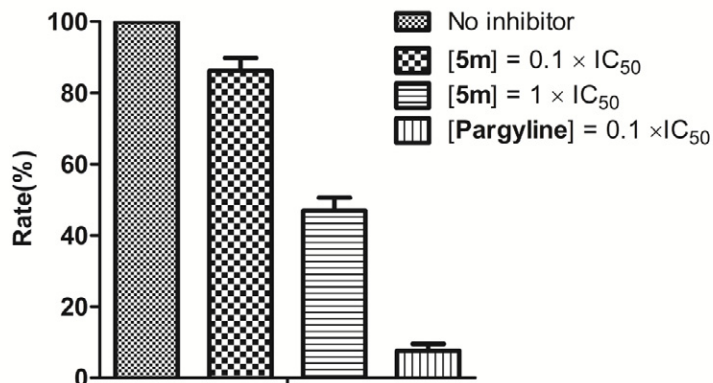


**Figure 4** Recovery of enzyme activity after dilution. Human MAO-B were preincubated with compound **5m** at concentrations equal to  $10 \times IC_{50}$  and  $100 \times IC_{50}$  for 30 min and then diluted to  $0.1 \times IC_{50}$  and  $1 \times IC_{50}$ , respectively. The residual enzyme activities were subsequently measured.

To further characterize the interaction of compound **5m** with MAO-B, the type of enzyme inhibition was also determined by enzyme kinetic study. The initial rates of the MAO-B-catalyzed oxidation of the substrate *p*-tyramine, applied at six different concentrations, were measured in the presence of three different concentrations of compound **5m**. The results are depicted as double reciprocal Lineweaver–Burk plots in Figure 5. The plots for compound **5m** were linear and intersected at the y-axis with the plot for the uninhibited enzyme. These results led us to conclude that the compound **5m** was competitive inhibitor, which occupies the substrate binding site of MAO-B, in agreement with its reversible mode of interaction.



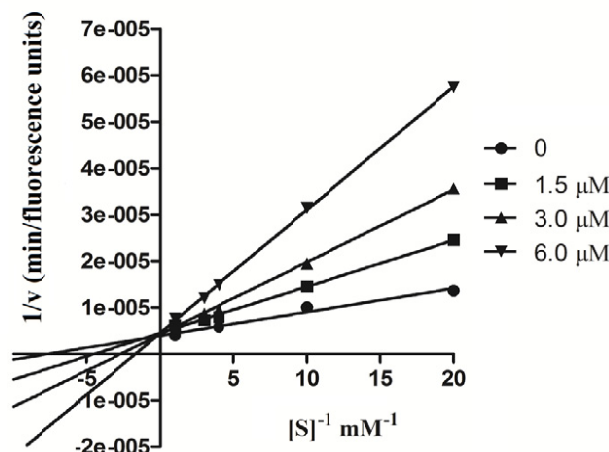


**Figure 5** Kinetic study on the mechanism of human MAO-B inhibition by compound **5m**. Overlaid Lineweaver–Burk reciprocal plots of the inhibition of human MAO-B in the presence of different concentrations of **5m** with *p*-tyramine (0.05–3.0 mM) as substrate are shown.

## 2.6. Docking Study

To study the binding modes of compound **5m** with AChE and MAO-B, docking study was carried out using the Molecular Operating Environment (MOE 2008.10) software package, and the Marvin software package [<http://www.chemaxon.com>] was performed to calculate the protonation level of the ligand in physiological pH.

### 2.6.1 Docking Study of Compounds **5m** with AChE

The binding mode of compound **5m** with respect to AChE was investigated based on the X-ray crystal structure of the recombinant human acetylcholinesterase in complex with donepezil (PDB code 4EY7)[54]. As shown in Figure 6, the coumarin moiety binds to the PAS of the enzyme, establishing a  $\pi$ - $\pi$  stacking interaction between its phenyl ring and the indole ring of Trp 286 (3.59 Å distance). Besides, the



using the ligand interactions application in MOE.

### 2.6.2 Docking Study of Compounds **5m** with MAO-B

The binding mode of compound **5m** with respect to MAO-B was investigated based on the X-ray crystal structure of the human monoamine oxidase B in complex with 7-(3-chlorobenzoyloxy)-4-(methylamino)methyl-coumarin (PDB code 2V61)[55]. It can be seen from the Figure 7 that coumarin moiety occupy the substrate cavity, which left the lactone function close to the FAD cofactor, and it was stabilized by hydrophobic interactions with Tyr 398, Phe 343 and Tyr 435. The *N*-benzylpiperidine moiety was located into entrance cavity and interacted with Thr 201, Thr 202, Phe 168, Leu 167, Leu 164, Pro 102, Pro 103, Ile 199 through van der waals and hydrophobic interactions.



(PAMPA-BBB). This model was established by Di et al. [56], which is a simple and rapid method to predict passive BBB permeation. The in vitro permeabilities ( $P_e$ ) of compound **5m** and 9 commercial drugs through a lipid extract of porcine brain were determined using PBS/EtOH (70:30). Assay validation was made by comparing the experimental permeability with the reported values of these commercial drugs (Table 4), which gave a good lineal correlation,  $P_e$  (exp.) = 1.2086  $P_e$  (bibl.) - 0.2915 ( $R^2 = 0.9260$ ). From this equation and taking into account the limit established by Di et al. for BBB permeation, we determined that compounds with permeabilities above  $4.54 \times 10^{-6} \text{ cm s}^{-1}$  could cross the BBB. Compound **5m** showed a  $P_e$  value of  $16.21 \times 10^{-6} \text{ cm s}^{-1}$ , which indicated that it could cross the BBB and reach the therapeutic targets in the CNS.

**Table 4.** Permeability ( $P_e \times 10^{-6} \text{ cm s}^{-1}$ ) in the PAMPA-BBB assay for compound **5m** and 9 commercial drugs used in the experiment validation.

compd	Bibliography <sup>a</sup>	Experiment <sup>b</sup>
<b>Testosterone</b>	17	16.81 ± 1.23
<b>Verapamil</b>	16	21.01 ± 0.75
<b><math>\beta</math>-Estradiol</b>	12	17.03 ± 0.44
<b>Clonidine</b>	5.3	8.14 ± 0.26
<b>Corticosterone</b>	5.1	3.11 ± 0.32
<b>Piroxicam</b>	2.5	1.32 ± 0.07
<b>Hydrocortisone</b>	1.9	1.41 ± 0.14
<b>Lomefloxacin</b>	1.1	1.81 ± 0.22
<b>Ofloxacin</b>	0.8	1.31 ± 0.01
<b>5m</b>		16.21 ± 0.21

<sup>a</sup> Taken from Ref.56. <sup>b</sup> Data are the mean ± SD of three independent experiments.

### 2.8. SH-SY5Y Neuroblastoma Cell Toxicity

In addition to the above biological evaluation, the potential cytotoxicity effect of compound **5m** on the human neuroblastoma cell line SH-SY5Y was also evaluated. After exposing the cells to this compound for 24 h, the cell viability was determined by the 3-(4, 5-dimethylthiazol-2-yl)-2, 5-diphenyltetrazolium (MTT) assay [57, 58]. The result indicated that **5m** show negligible cell death at 1-50  $\mu\text{M}$  (1  $\mu\text{M}$ :  $99.6 \pm 1.7$  %; 5  $\mu\text{M}$ :  $101.7 \pm 10.3$  %; 10  $\mu\text{M}$ :  $97.5 \pm 10.1$  %; 25  $\mu\text{M}$ :  $94.6 \pm 9.6$  %; 50  $\mu\text{M}$ :  $92.6 \pm 2.6$  %), which suggested that **5m** was nontoxic to SH-SY5Y cells and might be a suitable multi-target agent for the treatment of AD.

### 2.9. Hepatotoxicity of Compound 5m on HepG2 Cells

Finally, to verify whether the replacement of tacrine with *N*-benzylpiperidine moiety could eliminate the hepatotoxicity, an in vitro hepatotoxicity assay for compound **5m** was performed on HepG2 cells [59]. After 24 h incubation at 6.25-50  $\mu\text{M}$ , no obvious variation in cell viability was found for compound **5m** (6.25  $\mu\text{M}$ :  $100.7 \pm 2.3$  %; 12.5  $\mu\text{M}$ :  $101.4 \pm 2.1$  %; 25  $\mu\text{M}$ :  $105.1 \pm 6.1$  %; 50  $\mu\text{M}$ :  $104.2 \pm 5.3$  %), which indicated **5m** did not show hepatotoxicity on HepG2 cells and the replacement design was rational.

## 3. Conclusion

A series of donepezil-coumarin hybrids with ChEs and MAO-B inhibitory activity as multi-target agents have been designed and synthesized. Most of these compounds showed sub-micro to micromolar inhibitory activity toward AChE and BuChE, and clearly selective inhibition for MAO-B. Among these compounds,

compound **5m** presenting the most potent inhibition for animal ChEs and efficient inhibition for hChEs and hMAO-B was selected as the most promising compound for kinetic and molecular modeling studies. The results revealed that **5m** was a mixed-type inhibitor, binding simultaneously to CAS, PAS and mid-gorge site of AChE, and it was also a competitive inhibitor, which occupied the active site of eqBuChE and MAO-B. In addition, **5m** showed no toxicity to SH-SY5Y cells at 1-50  $\mu\text{M}$ , good ability to penetrate the CNS and no hepatotoxicity on HepG2 cells. Overall, all these biological properties highlighted the hybrid **5m** as a potential multi-target agent for the treatment of AD.

#### 4. Experimental section

##### 4.1. Chemistry

All chemical reagents used in synthesis were obtained from Sinopharm Chemical Reagent Co., Ltd. (China). The reactions were monitored by TLC on glass-packed precoated silica gel GF<sub>254</sub> (Qingdao Haiyang Chemical Plant, Qingdao, China) plates. Column chromatography was performed on silica gel (90-150  $\mu\text{m}$ ; Qingdao Marine Chemical Inc.). <sup>1</sup>H NMR spectra (500 MHz) and <sup>13</sup>C NMR spectra (125 MHz) were recorded on a Bruker ACF-500 spectrometer at 25°C. Chemical shifts are reported in ppm ( $\delta$ ) using the TMS as internal standard, and the coupling constants are reported in hertz (Hz). The purity of all compounds for biological evaluation was confirmed to > 95% by analytical HPLC conducted on an Agilent 1200 HPLC System. Mass spectra were carried out on a MS Agilent 1100 Series LC/MSD Trap mass spectrometer (ESI-MS) and an Agilent 6520B Q-TOF spectrometer (HR-ESI-MS), respectively.

## 4.2. General procedure for the preparation of compounds 5a-m and 9a-b.

A mixture of **4a-b** (1.5 mmol) and the corresponding coumarin derivatives **3a-l/8** (1.6 mmol) in dry acetonitrile (15 mL) was refluxed in the presence of anhydrous  $K_2CO_3$  (1.7 mmol) for 8 h. After cooling to the room temperature, the mixture was filtered, and the filtrate was evaporated under reduced pressure. The residue was purified by silica gel chromatography using  $CHCl_3/MeOH$  (50:1) as eluent to obtain target compounds **5a-m** as yellow oil.

### 4.2.1. 7-(2-((1-benzylpiperidin-4-yl)amino)ethoxy)-2H-chromen-2-one (5a).

Yield 69.1 %.  $^1H$  NMR (500 MHz, DMSO)  $\delta$  7.98 (d,  $J = 9.5$  Hz, 1H), 7.61 (d,  $J = 8.5$  Hz, 1H), 7.33 – 7.25 (m, 4H), 7.23 (d,  $J = 7.0$  Hz, 1H), 6.98 (d,  $J = 2.0$  Hz, 1H), 6.94 (dd,  $J = 8.5, 2.0$  Hz, 1H), 6.27 (d,  $J = 9.5$  Hz, 1H), 4.10 (t,  $J = 5.5$  Hz, 2H), 3.42 (s, 2H), 2.92 (t,  $J = 5.5$  Hz, 2H), 2.74 (d,  $J = 11.5$  Hz, 2H), 2.48 – 2.41 (m, 1H), 1.94 (t,  $J = 11.0$  Hz, 2H), 1.78 (d,  $J = 11.5$  Hz, 2H), 1.26 (td,  $J = 13.5, 3.5$  Hz, 2H).  $^{13}C$  NMR (125 MHz, DMSO)  $\delta$  162.28, 160.78, 155.87, 144.79, 139.12, 129.96, 129.21, 129.21, 128.58, 128.58, 127.26, 113.22, 112.94, 112.85, 101.74, 68.96, 62.68, 54.80, 52.28, 52.28, 45.28, 32.48, 32.48. ESI/MS  $m/z$ : 379.2  $[M + H]^+$ ; HRMS: calcd for  $C_{23}H_{27}N_2O_3$   $[M + H]^+$  379.2016, found 379.2013.

### 4.2.2. 7-(3-((1-benzylpiperidin-4-yl)amino)propoxy)-2H-chromen-2-one (5b).

Yield 68.2 %.  $^1H$  NMR (500 MHz, DMSO)  $\delta$  8.01 (d,  $J = 9.5$  Hz, 1H), 7.64 (d,  $J = 8.5$  Hz, 1H), 7.38 – 7.27 (m, 5H), 7.25 (t,  $J = 7.0$  Hz, 1H), 7.00 (d,  $J = 2.0$  Hz, 1H), 6.96 (dd,  $J = 8.5, 2.0$  Hz, 1H), 6.30 (d,  $J = 9.5$  Hz, 1H), 4.15 (t,  $J = 6.0$  Hz, 2H), 3.44 (s, 3H), 2.75 (dd,  $J = 14.0, 8.0$  Hz, 4H), 2.47 (d,  $J = 10.0$  Hz, 1H), 1.95 (t,  $J = 11.5$  Hz,



2H), 1.92 – 1.85 (m, 2H), 1.80 (d,  $J = 10.0$  Hz, 2H), 1.35-1.21 (m, 2H).  $^{13}\text{C}$  NMR (125 MHz, DMSO)  $\delta$  161.92, 160.46, 155.57, 144.49, 138.84, 129.67, 128.91, 128.91, 128.25, 128.25, 126.93, 112.92, 112.67, 112.58, 101.48, 67.96, 62.71, 53.46, 47.89, 46.71, 36.07, 33.33, 32.20, 32.20. ESI/MS  $m/z$ : 393.2  $[\text{M} + \text{H}]^+$ ; HRMS: calcd for  $\text{C}_{24}\text{H}_{29}\text{N}_2\text{O}_3$   $[\text{M} + \text{H}]^+$  393.2173, found 393.217.

**4.2.3. 7-(2-((2-(1-benzylpiperidin-4-yl)ethyl)amino)ethoxy)-2H-chromen-2-one (5c).**

Yield 67.3 %.  $^1\text{H}$  NMR (500 MHz, DMSO)  $\delta$  8.01 (d,  $J = 9.5$  Hz, 1H), 7.64 (d,  $J = 8.5$  Hz, 1H), 7.36–7.26 (m, 4H), 7.25 (d,  $J = 7.0$  Hz, 2H), 7.01 (s, 1H), 6.97 (d,  $J = 10.5$  Hz, 1H), 6.30 (t,  $J = 9.5$  Hz, 1H), 4.14 (t,  $J = 5.5$  Hz, 3H), 3.42 (s, 2H), 2.92 (t,  $J = 5.0$  Hz, 3H), 2.76 (d,  $J = 11.0$  Hz, 2H), 2.61 (t,  $J = 7.0$  Hz, 2H), 1.87 (t,  $J = 11.0$  Hz, 2H), 1.60 (d,  $J = 12.0$  Hz, 2H), 1.37 (dd,  $J = 13.5, 7.0$  Hz, 2H), 1.19-1.04 (m, 2H).  $^{13}\text{C}$  NMR (125MHz, DMSO)  $\delta$  162.22, 160.76, 155.87, 144.79, 139.14, 129.97, 129.21, 129.21, 128.55, 128.55, 27.23, 113.22, 112.97, 112.88, 101.78, 68.26, 63.01, 53.76, 53.76, 48.19, 47.01, 36.37, 33.63, 32.50, 32.50. ESI/MS  $m/z$ : 407.2  $[\text{M} + \text{H}]^+$ ; HRMS: calcd for  $\text{C}_{25}\text{H}_{31}\text{N}_2\text{O}_3$   $[\text{M} + \text{H}]^+$  407.2329, found 407.2328.

**4.2.4. 7-(2-((1-benzylpiperidin-4-yl)amino)ethoxy)-4-methyl-2H-chromen-2-one (5d).**

Yield 66.4 %.  $^1\text{H}$  NMR (500 MHz, DMSO)  $\delta$  7.66 (d,  $J = 9.5$  Hz, 1H), 7.36 – 7.25 (m, 4H), 7.22 (t,  $J = 7.0$  Hz, 1H), 6.99 – 6.91 (m, 2H), 6.19 (s, 1H), 4.10 (t,  $J = 5.5$  Hz, 2H), 3.42 (s, 2H), 2.92 (t,  $J = 5.5$  Hz, 2H), 2.74 (d,  $J = 11.5$  Hz, 2H), 2.48 – 2.41 (m, 1H), 2.38 (s, 3H), 1.94 (t,  $J = 10.5$  Hz, 2H), 1.78 (d,  $J = 11.5$  Hz, 2H), 1.32 –

1.18 (m, 2H).  $^{13}\text{C}$  NMR (125 MHz, DMSO)  $\delta$  162.17, 160.61, 155.21, 153.83, 139.14, 129.18, 128.56, 127.24, 126.88, 113.60, 112.90, 111.60, 101.74, 68.99, 62.70, 54.82, 52.30, 52.30, 45.33, 32.57, 32.57, 18.57. ESI/MS  $m/z$ : 392.2  $[\text{M} + \text{H}]^+$ ; HRMS: calcd for  $\text{C}_{24}\text{H}_{29}\text{N}_2\text{O}_3$   $[\text{M} + \text{H}]^+$  392.2173, found 392.2175.

**4.2.5. 7-(2-((1-benzylpiperidin-4-yl)amino)ethoxy)-4-chloro-2H-chromen-2-one (5e).**

Yield 65.2 %.  $^1\text{H}$  NMR (500 MHz, DMSO)  $\delta$  7.77 (d,  $J = 9.0$  Hz, 1H), 7.35 – 7.25 (m, 4H), 7.23 (t,  $J = 7.0$  Hz, 1H), 7.14 – 6.97 (m, 2H), 6.70 (s, 1H), 4.15 (t,  $J = 5.5$  Hz, 2H), 3.43 (s, 2H), 2.94 (t,  $J = 5.5$  Hz, 2H), 2.74 (d,  $J = 11.5$  Hz, 2H), 2.49 – 2.40 (m, 1H), 1.95 (t,  $J = 10.5$  Hz, 2H), 1.79 (d,  $J = 11.5$  Hz, 2H), 1.27 (td,  $J = 13.5$ , 3.5 Hz, 2H).  $^{13}\text{C}$  NMR (125 MHz, DMSO)  $\delta$  163.44, 159.16, 154.81, 149.06, 139.15, 129.18, 129.18, 129.18, 128.57, 128.57, 128.57, 127.25, 126.89, 113.91, 112.41, 111.35, 101.97, 69.29, 62.68, 54.80, 52.29, 52.29, 45.24, 32.53, 32.53. ESI/MS  $m/z$ : 413.1  $[\text{M} + \text{H}]^+$ ; HRMS: calcd for  $\text{C}_{23}\text{H}_{26}\text{ClN}_2\text{O}_3$   $[\text{M} + \text{H}]^+$  413.1626, found 413.1624.

**4.2.6. 7-(2-((1-benzylpiperidin-4-yl)amino)ethoxy)-4-methoxy-2H-chromen-2-one (5f).**

Yield 63.2 %.  $^1\text{H}$  NMR (500 MHz, DMSO)  $\delta$  7.69 (d,  $J = 9.0$  Hz, 1H), 7.37 – 7.27 (m, 4H), 7.25 (t,  $J = 7.0$  Hz, 1H), 6.99 (d,  $J = 2.0$  Hz, 1H), 6.95 (dd,  $J = 9.0$ , 2.0 Hz, 1H), 5.76 (s, 1H), 4.13 (t,  $J = 5.5$  Hz, 2H), 4.00 (s, 3H), 3.45 (s, 2H), 2.95 (t,  $J = 5.5$  Hz, 2H), 2.76 (d,  $J = 11.5$  Hz, 2H), 2.48 (dd,  $J = 9.0$ , 5.0 Hz, 1H), 1.97 (t,  $J = 10.8$  Hz, 2H), 1.81 (d,  $J = 11.0$  Hz, 2H), 1.29 (td,  $J = 13.5$ , 3.5 Hz, 2H).  $^{13}\text{C}$  NMR (125

MHz, DMSO)  $\delta$  166.71, 162.67, 162.51, 155.04, 139.11, 129.20, 129.20, 128.58, 128.58, 127.27, 124.41, 112.96, 108.81, 101.63, 88.12, 68.82, 62.65, 57.35, 54.82, 52.25, 45.22, 32.35. ESI/MS  $m/z$ : 409.2 [M + H]<sup>+</sup>; HRMS: calcd for C<sub>24</sub>H<sub>29</sub>N<sub>2</sub>O<sub>4</sub> [M + H]<sup>+</sup> 409.2122, found 409.2121.

**4.2.7. 7-(2-((1-benzylpiperidin-4-yl)amino)ethoxy)-4-ethoxy-2H-chromen-2-one (5g).**

Yield 60.6 %. <sup>1</sup>H NMR (500 MHz, DMSO)  $\delta$  7.68 (d,  $J$  = 9.0 Hz, 1H), 7.36 – 7.26 (m, 4H), 7.23 (t,  $J$  = 7.0 Hz, 1H), 6.99 – 6.91 (m, 2H), 5.71 (s, 1H), 4.24 (q,  $J$  = 7.0 Hz, 2H), 4.12 (t,  $J$  = 5.5 Hz, 2H), 3.44 (s, 2H), 2.96 (t,  $J$  = 5.5 Hz, 2H), 2.76 (d,  $J$  = 11.5 Hz, 2H), 2.48 (s, 1H), 1.96 (t,  $J$  = 11.0 Hz, 2H), 1.81 (d,  $J$  = 11.5 Hz, 2H), 1.42 (t,  $J$  = 7.0 Hz, 3H), 1.29 (dd,  $J$  = 20.5, 10.5 Hz, 2H). <sup>13</sup>C NMR (125 MHz, DMSO)  $\delta$  165.76, 162.59, 162.54, 155.07, 139.06, 129.19, 129.19, 128.57, 128.57, 127.27, 124.44, 112.92, 108.90, 101.57, 88.35, 68.66, 65.71, 62.62, 54.83, 53.30, 52.21, 45.17, 32.21, 14.40, 14.40. ESI/MS  $m/z$ : 423.2 [M + H]<sup>+</sup>; HRMS: calcd for C<sub>25</sub>H<sub>31</sub>N<sub>2</sub>O<sub>4</sub> [M + H]<sup>+</sup> 423.2278, found 409.228.

**4.2.8.**

**7-(2-((1-benzylpiperidin-4-yl)amino)ethoxy)-4-(trifluoromethyl)-2H-chromen-2-one (5h).**

Yield 68.5 %. <sup>1</sup>H NMR (500 MHz, DMSO)  $\delta$  7.64 (d,  $J$  = 8.5 Hz, 1H), 7.31 (dd,  $J$  = 13.5, 7.0 Hz, 5H), 7.26 (d,  $J$  = 6.5 Hz, 1H), 7.18 (s, 1H), 7.09 (d,  $J$  = 9.0 Hz, 1H), 6.88 (s, 1H), 4.18 (s, 2H), 3.46 (s, 2H), 2.99 (s, 2H), 2.78 (d,  $J$  = 11.0 Hz, 2H), 1.99 (dd,  $J$  = 25.0, 10.5 Hz, 3H), 1.83 (d,  $J$  = 12.0 Hz, 2H), 1.34 - 1.25 (m, 2H). <sup>13</sup>C NMR

(125 MHz, DMSO)  $\delta$  162.70, 159.17, 159.12, 156.33, 138.50, 129.28, 129.28, 129.19, 128.62, 128.62, 127.39, 126.37, 114.21, 113.76, 107.03, 102.76, 68.08, 68.08, 62.42, 52.00, 52.00, 44.76, 31.39, 29.47. ESI/MS  $m/z$ : 447.2 [M + H]<sup>+</sup>; HRMS: calcd for C<sub>24</sub>H<sub>26</sub>F<sub>3</sub>N<sub>2</sub>O<sub>3</sub> [M + H]<sup>+</sup> 447.189, found 413.1888.

**4.2.9. 7-(2-((1-benzylpiperidin-4-yl)amino)ethoxy)-4-phenyl-2H-chromen-2-one (5i).**

Yield 62.5 %. <sup>1</sup>H NMR (500 MHz, DMSO)  $\delta$  7.63 – 7.57 (m, 3H), 7.54 (dd,  $J$  = 7.0, 2.5 Hz, 2H), 7.36 (d,  $J$  = 9.0 Hz, 1H), 7.35 – 7.27 (m, 4H), 7.25 (t,  $J$  = 7.0 Hz, 1H), 7.11 (d,  $J$  = 2.5 Hz, 1H), 6.96 (dd,  $J$  = 9.0, 2.5 Hz, 1H), 6.26 (s, 1H), 4.15 (t,  $J$  = 5.5 Hz, 2H), 3.45 (s, 2H), 2.97 (t,  $J$  = 5.5 Hz, 2H), 2.77 (d,  $J$  = 11.5 Hz, 2H), 2.48 (d,  $J$  = 10.0 Hz, 1H), 1.97 (t,  $J$  = 10.5 Hz, 2H), 1.82 (d,  $J$  = 11.0 Hz, 2H), 1.28 (dt,  $J$  = 9.0, 8.0 Hz, 2H). <sup>13</sup>C NMR (125 MHz, DMSO)  $\delta$  162.28, 160.45, 155.95, 155.64, 139.08, 135.50, 130.13, 129.34, 129.34, 129.20, 129.20, 128.89, 128.89, 128.58, 128.58, 128.32, 127.27, 113.28, 112.33, 111.82, 102.26, 68.83, 62.63, 54.82, 52.23, 52.23, 45.19, 32.27, 32.27. ESI/MS  $m/z$ : 455.2 [M + H]<sup>+</sup>; HRMS: calcd for C<sub>29</sub>H<sub>31</sub>N<sub>2</sub>O<sub>3</sub> [M + H]<sup>+</sup> 455.2329, found 455.2327.

**4.2.10. 7-(2-((1-benzylpiperidin-4-yl)amino)ethoxy)-3-methyl-2H-chromen-2-one (5j).**

Yield 64.1 %. <sup>1</sup>H NMR (500 MHz, DMSO)  $\delta$  7.80 (s, 1H), 7.52 (d,  $J$  = 8.5 Hz, 1H), 7.35 – 7.26 (m, 4H), 7.23 (t,  $J$  = 7.0 Hz, 1H), 6.96 (d,  $J$  = 2.0 Hz, 1H), 6.92 (dd,  $J$  = 8.5, 2.5 Hz, 1H), 4.09 (t,  $J$  = 5.5 Hz, 2H), 3.43 (s, 2H), 2.91 (t,  $J$  = 5.5 Hz, 2H), 2.74 (d,  $J$  = 11.5 Hz, 2H), 2.48 – 2.40 (m, 1H), 2.06 (s, 3H), 1.95 (t,  $J$  = 11.0 Hz, 2H),

1.79 (d,  $J = 11.5$  Hz, 2H), 1.31 – 1.20 (m, 2H).  $^{13}\text{C}$  NMR (125 MHz, DMSO)  $\delta$  162.02, 161.24, 154.80, 140.25, 139.15, 129.19, 129.19, 128.93, 128.93, 128.56, 127.24, 121.52, 113.35, 113.05, 101.44, 68.94, 62.70, 54.80, 52.30, 45.36, 32.58, 32.58, 16.91. ESI/MS  $m/z$ : 393.2  $[\text{M} + \text{H}]^+$ ; HRMS: calcd for  $\text{C}_{24}\text{H}_{26}\text{F}_3\text{N}_2\text{O}_3$   $[\text{M} + \text{H}]^+$  393.2173, found 393.2174.

#### 4.2.11.

#### 7-(2-((1-benzylpiperidin-4-yl)amino)ethoxy)-3,4-dimethyl-2H-chromen-2-one

#### (5k).

Yield 68.2 %.  $^1\text{H}$  NMR (500 MHz, DMSO)  $\delta$  7.74 – 7.64 (m, 1H), 7.38 – 7.27 (m, 4H), 7.25 (t,  $J = 7.0$  Hz, 1H), 6.96 (dd,  $J = 5.5, 2.5$  Hz, 2H), 4.10 (t,  $J = 5.5$  Hz, 2H), 3.44 (s, 2H), 2.93 (t,  $J = 5.5$  Hz, 2H), 2.76 (d,  $J = 11.5$  Hz, 2H), 2.45 (t,  $J = 10.0$  Hz, 1H), 2.37 (s, 3H), 2.09 (s, 3H), 1.97 (t,  $J = 11.0$  Hz, 2H), 1.80 (d,  $J = 11.5$  Hz, 2H), 1.27 (d,  $J = 11.5$  Hz, 2H).  $^{13}\text{C}$  NMR (125 MHz, DMSO)  $\delta$  161.71, 161.14, 153.50, 147.28, 139.21, 129.17, 129.17, 128.56, 128.56, 127.23, 126.60, 118.32, 114.08, 112.78, 101.46, 100.09, 69.02, 62.72, 54.81, 52.34, 45.43, 32.73, 15.36, 13.36. ESI/MS  $m/z$ : 407.2  $[\text{M} + \text{H}]^+$ ; HRMS: calcd for  $\text{C}_{25}\text{H}_{31}\text{N}_2\text{O}_3$   $[\text{M} + \text{H}]^+$  407.2329, found 407.2327.

#### 4.1.12.

#### 7-(2-((1-benzylpiperidin-4-yl)amino)ethoxy)-3-chloro-4-methyl-2H-chromen-2

#### -one (5l).

Yield 68.3 %.  $^1\text{H}$  NMR (500 MHz, DMSO)  $\delta$  7.75 (t,  $J = 15.0$  Hz, 1H), 7.31 – 7.22 (m, 4H), 7.20 (t,  $J = 7.0$  Hz, 1H), 7.04 – 6.95 (m, 2H), 4.10 (t,  $J = 5.0$  Hz, 2H),

3.40 (s, 2H), 2.92 (t,  $J = 5.0$  Hz, 2H), 2.72 (d,  $J = 11.0$  Hz, 2H), 2.47 (s, 3H), 2.47-2.39 (m, 1H), 1.92 (t,  $J = 11.0$  Hz, 2H), 1.77 (d,  $J = 11.5$  Hz, 2H), 1.24 – 1.16 (m, 2H).  $^{13}\text{C}$  NMR (125 MHz, DMSO)  $\delta$  160.73, 156.83, 153.09, 152.99, 149.29, 129.61, 129.61, 128.53, 128.53, 127.58, 117.22, 113.95, 113.75, 102.25, 101.74, 79.39, 79.01, 63.16, 62.74, 52.34, 45.32, 29.34, 29.34, 16.60. ESI/MS  $m/z$ : 427.2  $[\text{M} + \text{H}]^+$ ; HRMS: calcd for  $\text{C}_{24}\text{H}_{28}\text{ClN}_2\text{O}_3$   $[\text{M} + \text{H}]^+$  427.1783, found 427.1781.

#### 4.1.13.

#### 3-(2-((1-benzylpiperidin-4-yl)amino)ethoxy)-7,8,9,10-tetrahydro-6H-benzo[c]chromen-6-one (5m).

Yield 65.1 %.  $^1\text{H}$  NMR (500 MHz, DMSO)  $\delta$  7.60 (d,  $J = 9.5$  Hz, 1H), 7.34 – 7.25 (m, 4H), 7.23 (t,  $J = 7.0$  Hz, 1H), 6.97 – 6.87 (m, 2H), 4.10 (t,  $J = 5.5$  Hz, 2H), 3.43 (s, 2H), 2.94 (t,  $J = 5.5$  Hz, 2H), 2.82 – 2.68 (m, 4H), 2.47 (t,  $J = 10.0$  Hz, 1H), 2.40 (t,  $J = 6.0$  Hz, 2H), 1.95 (t,  $J = 11.0$  Hz, 2H), 1.88 – 1.58 (m, 6H), 1.33 – 1.20 (m, 2H).  $^{13}\text{C}$  NMR (125 MHz, DMSO)  $\delta$  161.35, 160.99, 153.44, 147.99, 139.14, 129.18, 129.18, 128.57, 128.57, 127.25, 125.40, 119.93, 113.63, 112.71, 101.56, 68.76, 62.67, 54.84, 52.27, 45.32, 32.46, 32.46, 25.12, 24.02, 21.70, 21.35. ESI/MS  $m/z$ : 427.2  $[\text{M} + \text{H}]^+$ ; HRMS: calcd for  $\text{C}_{24}\text{H}_{28}\text{ClN}_2\text{O}_3$   $[\text{M} + \text{H}]^+$  427.1783, found 427.1781.

#### 4.1.14. 7-(((1-benzylpiperidin-4-yl)amino)methyl)-4-methyl-2H-chromen-2-one (9a).

Yield 64.6 %.  $^1\text{H}$  NMR (500 MHz, DMSO)  $\delta$  7.72 (d,  $J = 8.0$  Hz, 1H), 7.38 (d,  $J = 9.0$  Hz, 2H), 7.31 (dt,  $J = 14.5, 7.0$  Hz, 4H), 7.25 (t,  $J = 7.0$  Hz, 1H), 6.36 (s, 1H), 3.86 (s, 2H), 3.44 (s, 2H), 2.75 (d,  $J = 12.0$  Hz, 2H), 2.44 (s, 3H), 2.48 – 2.35 (m, 1H),

1.93 (t,  $J = 11.0$  Hz, 2H), 1.81 (d,  $J = 11.0$  Hz, 2H), 1.33 (td,  $J = 13.5, 3.0$  Hz, 2H).

$^{13}\text{C}$  NMR (125MHz, DMSO)  $\delta$  160.39, 153.65, 153.51, 146.78, 139.06, 129.18, 129.18, 128.57, 128.57, 127.26, 125.48, 124.46, 118.58, 115.78, 114.09, 62.63, 54.00, 52.22, 52.22, 49.48, 32.35, 32.35, 18.53. ESI/MS  $m/z$ : 363.2  $[\text{M} + \text{H}]^+$ ; HRMS: calcd for  $\text{C}_{23}\text{H}_{27}\text{N}_2\text{O}_2$   $[\text{M} + \text{H}]^+$  363.2067, found 363.2068.

#### 4.1.15.

**7-(((2-(1-benzylpiperidin-4-yl)ethyl)amino)methyl)-4-methyl-2H-chromen-2-one (9b).**

Yield 67.3 %.  $^1\text{H}$  NMR (500 MHz, DMSO)  $\delta$  7.70 (d,  $J = 8.5$  Hz, 1H), 7.33 (d,  $J = 7.5$  Hz, 2H), 7.29 (dt,  $J = 14.0, 7.0$  Hz, 4H), 7.22 (t,  $J = 7.0$  Hz, 1H), 6.34 (s, 1H), 3.78 (s, 2H), 3.40 (s, 2H), 2.74 (d,  $J = 11.0$  Hz, 2H), 2.48 (t,  $J = 7.0$  Hz, 2H), 2.42 (s, 3H), 1.86 (t,  $J = 11.0$  Hz, 2H), 1.56 (d,  $J = 12.0$  Hz, 2H), 1.36 (dd,  $J = 14.0, 7.0$  Hz, 2H), 1.29 (t,  $J = 14.0$  Hz, 1H), 1.15 – 1.03 (m, 2H).  $^{13}\text{C}$  NMR (125 MHz, DMSO)  $\delta$  160.38, 153.64, 153.53, 146.41, 139.16, 129.18, 129.18, 128.54, 128.54, 127.21, 125.50, 124.49, 118.62, 115.81, 114.12, 63.00, 53.78, 52.69, 46.48, 36.63, 33.69, 32.56, 18.53. ESI/MS  $m/z$ : 391.2  $[\text{M} + \text{H}]^+$ ; HRMS: calcd for  $\text{C}_{25}\text{H}_{31}\text{ClN}_2\text{O}_2$   $[\text{M} + \text{H}]^+$  391.238, found 391.2383.

## 5. Biological Evaluation.

### 5.1. Inhibition Experiments of ChEs

Acetylcholinesterase (AChE, E.C. 3.1.1.7) from electric eel and human erythrocytes, butylcholinesterase (BuChE, E.C. 3.1.1.8) from equine serum and human serum, S-butylthiocholine iodide (BTCl), acetylthiocholine iodide (ATCl), 5,

5'-dithiobis-(2-nitrobenzoic acid) (Ellman's reagent, DTNB), donepezil and tacrine hydrochloride were purchased from Sigma-Aldrich (St. Louis, MO, USA). The inhibitory activities of test compounds **5a-m** and **9a-b** was evaluated by Ellman's method [45]. The compounds were dissolved in DMSO and diluted with the buffer solution (50 mM Tris-HCl, pH = 8.0, 0.1 M NaCl, 0.02 M MgCl<sub>2</sub>·6H<sub>2</sub>O) to yield corresponding test concentrations (DMSO less than 0.01%). In each well of the plate, 160  $\mu$ L of 1.5 mM DTNB, 50  $\mu$ L of AChE (0.22 U/mL *ee*AChE or 0.05 U/mL hAChE) or 50  $\mu$ L of BuChE (0.12 U/mL *eq*BuChE or 0.024 U/mL hBuChE) were incubated with 10  $\mu$ L of different concentrations of test compounds (0.001-100  $\mu$ M) at 37 °C for 6 min. After this period, acetylthiocholine iodide (15 mM) or S-butyrylthiocholine iodide (15 mM) as the substrate (30  $\mu$ L) was added and the absorbance was measured with a wavelength of 405 nm at different time intervals (0, 60, 120, and 180 s). IC<sub>50</sub> values were calculated as concentration of compound that produces 50% enzyme activity inhibition, using the Graph Pad Prism 4.03 software (San Diego, CA, USA). Results are expressed as the mean  $\pm$  SD of at least three different experiments performed in triplicate.

## 5.2. Inhibition Experiments of MAOs

The inhibitory activities of the test compounds on hMAOs were determined by a fluorimetric method according to a previously described protocol [50, 51]. The Amplex Red assay kit used to measure the production of H<sub>2</sub>O<sub>2</sub> from substrate *p*-tyramine was purchased from Molecular Probes, Inc. (Eugene, Oregon, USA) and recombinant hMAO-A and hMAO-B was obtained from Sigma-Aldrich (St. Louis,



MO, USA).

### 5.3. Kinetic Study of ChE Inhibition

The kinetic study of ChE was performed by Ellman's method with three different concentrations (0.44, 0.87 and 1.74  $\mu\text{M}$ ) of compound **5m**. Lineweaver–Burk reciprocal plots were constructed by plotting  $1/\text{velocity}$  against  $1/[\text{substrate}]$  at varying concentrations of the substrate acetylthiocholine (0.05–0.5 mM). The plots were assessed by a weighted least-squares analysis that assumed the variance of velocity ( $v$ ) to be a constant percentage of  $v$  for the entire data set. Data analysis was performed with Graph Pad Prism 4.03 software (San Diego, CA, USA).

### 5.4. Reversibility of Monoamine Oxidase B Inhibition

The reversibility of MAO-B inhibition was determined by dilution assay [53]. At concentrations equal to  $10 \times \text{IC}_{50}$  and  $100 \times \text{IC}_{50}$  for hMAO-B inhibition, compound **5m** was incubated with the enzyme (0.75 mg/ml) for 30 min at 37 °C in PBS (0.05 M, pH 7.4). The parallel control was conducted by replacing the compound with buffer, and the corresponding amount of DMSO was added as co-solvent to all incubations. After the incubation period, the complex was diluted 100-fold to obtain final concentrations of compound **5m** equal to  $0.1 \times \text{IC}_{50}$  and  $1 \times \text{IC}_{50}$ . For comparison, pargyline were incubated with hMAO-B at concentrations of  $10 \times \text{IC}_{50}$  in similar manner and diluted to  $0.1 \times \text{IC}_{50}$ . The residual enzyme catalytic rates were determined following the method for the  $\text{IC}_{50}$  determination and all results were expressed as mean  $\pm$  SD.

### 5.5. Kinetic Study of MAO-B Inhibition

The type of MAO-B inhibition was determined by constructing a set of Lineweaver–Burk plots. Six different concentrations of the substrate *p*-tyramine was applied, and the initial catalytic rates of hMAO-B were measured in the absence and in the presence of three different concentrations (1.5, 3.0 and 6.0  $\mu\text{M}$ ) of compound **5m**. The assay conditions and measurements were similar to the  $\text{IC}_{50}$  determination. Linear regression analysis was carried out using Graph Pad Prism 4.03 software (San Diego, CA, USA).

### 5.6. Docking study

Molecular docking studies were performed using Molecular Operating Environment (MOE) software version 2008.10 (Chemical Computing Group, Montreal, Canada). The X-ray crystallographic structures of human AChE (hAChE) in complex with donepezil (PDB code 4EY7) and human MAO-B in complex with 7-(3-chlorobenzyloxy)-4-(methylamino)methyl-coumarin (PDB code 2V61) were obtained from the PDB. Hydrogens and partial charges were added using protonate 3D application in MOE. The compound **5m** was constructed using the MOE builder module and energy minimized using Merck Molecular force field (MMFF94x, RMSD gradient:  $0.05 \text{ kcal mol}^{-1} \text{ \AA}^{-1}$ ). The protonation level of the compound in physiological pH was calculated by the Marvin 16.2.8.0 2016 software package, ChemAxon [<http://www.chemaxon.com>]. The MOE Dock application was used for docking **5m** into the active site of the corresponding protein. The poses were generated by the Triangle Matcher placement method and then were rescored using ASE scoring function. The Forcefiled was selected as the refinement method. The retained best poses were

visually inspected and the interactions with binding pocket residues were analyzed.

### 5.7. In Vitro Blood-Brain Barrier Permeation Assay

The ability of test compounds that penetrate into brain was evaluated using a parallel artificial membrane permeation assay (PAMPA) for blood-brain-barrier according to the method established by Di et al.[56]. Commercial drugs, PBS (pH = 7.4), DMSO and dodecane were obtained from Sigma and Aladdin. Porcine brain lipid (PBL) was purchased from Avanti Polar Lipids. The donor microplate (96-well filter plate, PVDF membrane, pore size is 0.45  $\mu\text{m}$ ) and the acceptor microplate (indented 96-well plate) were both from Millipore. The 96-well UV plate (COSTAR) was acquired from Corning Inc. The compound was firstly dissolved in DMSO at a concentration of 5 mg/mL. Then, it was diluted 200-fold with a mixture of PBS/EtOH (70:30) to give a final concentration of 25  $\mu\text{g/mL}$ . The filter membrane in donor microplate was coated with PBL dissolved in dodecane (4  $\mu\text{L}$ , 20 mg/mL). After that, 200  $\mu\text{L}$  of diluted solution and 300  $\mu\text{L}$  of PBS/EtOH (70:30) were added to the donor wells and the acceptor wells, respectively. The donor filter plate was carefully placed on the acceptor plate to make the underside of filter membrane can contact with buffer solution. After leaving this sandwich assembly undisturbedly for 16 h at 25  $^{\circ}\text{C}$ , the donor plate was carefully removed, and the concentrations of test compound in the acceptor, donor and reference wells were measured with a UV plate reader (SpectraMax Plus 384, Molecular Devices, Sunnyvale, CA, USA). Each sample was analyzed at least three independent runs in four wells, and the results are given as the means  $\pm$  SD.  $P_e$  was calculated using the following expression:  $P_e = \{-V_d V_a / [(V_d +$

$V_a)At\} \ln(1 - \text{drug}_{\text{acceptor}}/\text{drug}_{\text{equilibrium}})$ , where  $V_d$  is the volume of donor well,  $V_a$  is the volume in the acceptor well,  $A$  is the filter area,  $t$  is the permeation time,  $\text{drug}_{\text{acceptor}}$  is the absorbance obtained in the acceptor well, and  $\text{drug}_{\text{equilibrium}}$  is the theoretical equilibrium absorbance. A plot of the experimental  $P_e$  values of 9 standard drugs versus their bibliographic values provided a good linear correlation,  $P_e(\text{exp.}) = 1.2086 P_e(\text{bibl.}) - 0.2915$  ( $R^2 = 0.9260$ ) (Supporting Information, Figure S1).

### 5.8. SH-SY5Y Neuroblastoma Cell Toxicity

The cytotoxicity effect of test compound on the human neuroblastoma SH-SY5Y cells was evaluated by MTT assay according to a described methods [57, 58]. The SH-SY5Y cells were grown in a 1:1 mixture of Eagle's minimum essential medium (EMEM) and ham's F-12 medium supplemented with 10% fetal bovine serum (FBS), 100 U/mL penicillin and 100  $\mu\text{g}/\text{mL}$  streptomycin in 5%  $\text{CO}_2$  at 37 °C. For cell viability assay, cells were placed into 96-well plates at a seeding density of 10000 cells/well and incubated with compound **5m** for 24 h. After this incubation, 20  $\mu\text{L}$  of MTT at 37 °C was added for 4 h. Then, the medium was removed, and 200  $\mu\text{L}$  of DMSO was added to dissolve the formazan crystal formed. The absorbance was measured in a microculture plate reader with a test wavelength of 570 nm and a reference wavelength of 630 nm. Results are expressed as the mean  $\pm$  SD of three independent experiments.

### 5.9. Hepatotoxicity of Compound **5m** on HepG2 Cells

The hepatotoxicity evaluation was performed on the human hepatocellular liver carcinoma cells (HepG2) by MTT assay according to a described method [59].

HepG2 cells were grown in DMEM supplemented with 10% FBS and 50 U/mL of penicillin at 37 °C in humidified atmosphere containing 5% CO<sub>2</sub>. For the experiments, cells (4000 cells/well) were seeded in 96-well plate in complete medium; after 24 h, the medium was removed and cells were exposed to the increasing concentrations of compound **5m** (6.25, 12.5, 25, 50 μM) in DMEM with no serum for further 24 h. Cell survival was measured through MTT assay.

### Acknowledgement

This research work was financially supported by Program for Changjiang Scholars and Innovative Research Team in University (IRT1193), A Project Funded by the Priority Academic Program Development of Jiangsu Higher Education Institutions (PAPD) and the Project of the National Natural Sciences Foundation of China (81573313).

### Reference

- [1] Querfurth, H. W.; LaFerla, F. M. *N. Engl. J. Med.* **2010**, *362*, 329.
- [2] Huang, Y.; Mucke, L. *Cell* **2012**, *148*, 1204.
- [3] Mount, C.; Downton, C. *Nat. Med.* **2006**, *12*, 780.
- [4] Ballard, C.; Gauthier, S.; Corbett, A.; Brayne, C.; Aarsland, D.; Jones, E. *Lancet* **2011**, *377*, 1019.
- [5] Scarpini, E.; Schelterns, P.; Feldman, H. *Lancet Neurol.* **2003**, *2*, 539.
- [6] Kumar, N. S.; Nisha, N. *Chin. J. Nat. Med.* **2014**, *12*, 801.
- [7] Muñoz-Torrero, D. *Curr. Med. Chem.* **2008**, *15*, 2433.
- [8] Anand, P.; Singh, B. *Arch. Pharm. Res.* **2013**, *36*, 375.

- [9] Kumar, A.; Singh, A.; Ekavali. *Pharmacol. Rep.* **2015**, *67*, 195.
- [10] Molano, J. R.; Bratt, R.; Shatz, R. *Curr. Treat. Options Neurol.* **2015**, *17*, 363.
- [11] Cavalli, A.; Bolognesi, M. L.; Minarini, A.; Rosini, M.; Tumiatti, V.; Recanatini, M.; Melchiorre, C. *J. Med. Chem.* **2008**, *51*, 347.
- [12] León, R.; Garcia, A. G.; Marco-Contelles, J. *Med. Res. Rev.* **2013**, *33*, 139.
- [13] Zimmermann, G. R.; Lehar, J.; Keith, C. T. *Drug Discov. Today* **2007**, *12*, 34.
- [14] Morphy, R.; Rankovic, Z. *J. Med. Chem.* **2005**, *48*, 6523.
- [15] Agis-Torres, A.; Solhuber, M.; Fernandez, M.; Sanchez-Montero, J. M. *Curr. Neuropharmacol* **2014**, *12*, 2.
- [16] Tumiatti, V.; Minarini, A.; Bolognesi, M. L.; Milelli, A.; Rosini, M.; Melchiorre, C. *Curr. Med. Chem.* **2010**, *17*, 1825.
- [17] Mitoma, J.; Ito, A. *J. Biochem.* **1992**, *111*, 20.
- [18] Greenawalt, J.W.; Schnaitman, C. *J. Cell. Biol.* **1970**, *46*, 173.
- [19] Carradori, S.; Petzer, J. P. *Expert Opin. Ther. Pat.* **2015**, *25*, 91.
- [20] Johnston, J. P. *Biochem. Pharmacol.* **1968**, *17*, 1285.
- [21] Grimsby, J.; Lan, N. C.; Neve, R.; Chen, K.; Shih, J. C. *J. Neurochem.* **1990**, *55*, 1166.
- [22] Danielczyk, W.; Streifler, M.; Konradi, C.; Riederer, P.; Moll, G. *Acta Psychiatr. Scand.* **1988**, *78*, 730.
- [23] Cai, Z. *Mol. Med. Rep.* **2014**, *9*, 1533.
- [24] Doraiswamy, P. M. *CNS Drugs* **2002**, *16*, 811.
- [25] Samadi, A.; de los Rios, C.; Bolea, I.; Chioua, M.; Iriepa, I.; Moraleda, I.;

Bartolini, M.; Andrisano, V.; Galvez, E.; Valderas, C.; Unzeta, M.; Marco-Contelles, J.

*Eur. J. Med. Chem.* **2012**, *52*, 251.

[26] Bolea, I.; Juárez-Jiménez, J.; de los Ríos, C.; Chioua, M.; Pouplana, R.; Luque, F.

J.; Unzeta, M.; Marco-Contelles, J.; Samadi, A. *J. Med. Chem.* **2011**, *54*, 8251.

[27] Bautista-Aguilera, O. M.; Samadi, A.; Chioua, M.; Nikolic, K.; Filipic, S.;

Agbaba, D.; Soriano, E.; de Andrés, L.; Rodríguez-Franco, M. I.; Alcaro, S.; Ramsay,

R.; Ortuso, F.; Yáñez, M.; Marco-Contelles, J. *J. Med. Chem.* **2014**, *57*, 10455.

[28] Bruhlmann, C.; Ooms, F.; Carrupt, P. A.; Testa, B.; Catto, M.; Leonetti, F.;

Altomare, C.; Carotti, A. *J. Med. Chem.* **2001**, *44*, 3195.

[29] Farina, R.; Pisani, L.; Catto, M.; Nicolotti, O.; Gadaleta, D.; Denora, N.;

Soto-Otero, R.; Mendez-Alvarez, E.; Passos, C. S.; Muncipinto, G.; Altomare, C. D.;

Nurisso, A.; Carrupt, P. A.; Carotti, A. *J. Med. Chem.* **2015**, *58*, 5561.

[30] Yáñez, M.; Viña, D. *Curr. Top Med. Chem.* **2013**, *13*, 1692.

[31] Sterling, J.; Herzig, Y.; Goren, T.; Finkelstein, N.; Lerner, D.; Goldenberg, W.;

Miskolczi, I.; Molnar, S.; Rantal, F.; Tamas, T.; Toth, G.; Zagyva, A.; Zekany, A.;

Finberg, J.; Lavian, G.; Gross, A.; Friedman, R.; Razin, M.; Huang, W.; Kraus, B.;

Chorev, M.; Youdim, M. B.; Weinstock, M. *J. Med. Chem.* **2005**, *45*, 5260.

[32] Wang, L.; Esteban, G.; Ojima, M.; Bautista-Aguilera, O. M.; Inokuchi, T.;

Moraleda, I.; Iriepa, I.; Samadi, A.; Youdim, M. B.; Romero, A.; Soriano, E.; Herrero,

R.; Fernandez Fernandez, A. P.; Ricardo Martinez, Murillo; Marco-Contelles, J.

Unzeta, M. *Eur. J. Med. Chem.* **2014**, *80*, 543.

[33] Pisani, L.; Catto, M.; Leonetti, F.; Nicolotti, O.; Stefanachi, A.; Campagna, F.;

Carotti, A. *Curr. Med. Chem.* **2011**, *18*, 4568.

[34] Sterling, J.; Herzig, Y.; Goren, T.; Finkelstein, N.; Lerner, D.; Goldenberg, W.;

Mikolczi, I.; Molnar, S.; Rantal, F.; Tamas, T.; Toth, G.; Zagyva, A.; Zekany, A.;

Finberg, J.; Lavian, G.; Gross, A.; Friedman, R.; Razin, M.; Huang, W.; Kraus, B.;

Chorev, M.; Youdim, M.B.; Weinstock, M. *J. Med. Chem.* **2002**, *45*, 5260.

[35] Xie, S. S.; Wang, X.; Jiang, N.; Yu, W.; Wang, K. D.; Lan, J. S.; Li, Z. R.; Kong,

L. Y. *Eur. J. Med. Chem.* **2015**, *95*, 153.

[36] Soukup, O.; Jun, D.; Zdarova-Karasova, J.; Patocka, J.; Musilek, K.; Korabecny,

J.; Krusek, J.; Kaniakova, M.; Sepsova, V.; Mandikova, J.; Trejtnar, F.; Pohanka, M.;

Drtinova, L.; Pavlik, M.; Tobin, G.; Kuca, K. *Curr. Alzheimer Res.* **2013**, *10*, 893.

[37] Sugimoto, H.; Yamanish, Y.; Iimura, Y.; Kawakami, Y. *Curr. Med. Chem.* **2000**, *7*,

303.

[38] Sepsova, V.; Karasova, J. Z.; Tobin, G.; Jun, D.; Korabecny, J.; Cabelova, P.;

Janska, K.; Krusek, J.; Skrenkova, K.; Kuca, K.; Soukup, O. *Gen. Physiol. Biophys.*

**2015**, *34*, 189.

[39] Fernández-Bachiller, M. I.; Pérez, C.; González-Muñoz, G. C.; Conde, S.; López,

M. G.; Villarroya, M.; García, A. G.; Rodríguez-Franco, M. I. *J. Med. Chem.* **2010**, *53*,

4927.

[40] Catto, M.; Pisani, L.; Leonetti, F.; Nicolotti, O.; Pesce, P.; Stefanachi, A.;

Cellamare, S.; Carotti, A. *Bioorg. Med. Chem.* **2013**, *21*, 146.

[41] Pisani, L.; Catto, M.; Giangreco, I.; Leonetti, F.; Nicolotti, O.; Stefanachi, A.;

Cellamare, S.; Carotti, A. *ChemMedChem.* **2010**, *5*, 1616.



- [42] Gnerre, C.; Catto, M.; Leonetti, F.; Weber, P.; Carrupt, P. A.; Altomare, C.; Carotti, A.; Testa, B. *J. Med. Chem.* **2000**, *43*, 4747.
- [43] Pisani, L.; Muncipinto, G.; Miscioscia, T. F.; Nicolotti, O.; Leonetti, F.; Catto, M.; Caccia, C.; Salvati, P.; Soto-Otero, R.; Mendez-Alvarez, E.; Passeleu, C.; Carotti, A. *J. Med. Chem.* **2000**, *52*, 6685.
- [44] Hill, B.; Liu, Y.; Taylor, S. D. *Org. Lett.* **2004**, *6*, 4285.
- [45] Ellman, G. L.; Courtney, K. D.; Andres, V., Jr.; Feather-Stone, R. M. *Biochem. Pharmacol.* **1961**, *7*, 88.
- [46] Venneri, A.; McGeown, W. J.; Shanks, M. F. *Neuroreport* **2005**, *16*, 107.
- [47] Giacobini, E. *Pharmacol. Res.* **2004**, *50*, 433.
- [48] Xie, S. S.; Lan, J. S.; Wang, X. B.; Jiang, N.; Dong, G.; Li, Z. R.; Wang, K. D.; Guo, P. P.; Kong, L. Y. *Eur. J. Med. Chem.* **2015**, *93*, 42.
- [49] Fernandez-Bachiller, M. I.; Perez, C.; Monjas, L.; Rademann, J.; Rodriguez-Franco, M. I. *J. Med. Chem.* **2012**, *55*, 1303.
- [50] Yáñez, M.; Fraiz, N.; Cano, E.; Orallo, F. *Biochem. Biophys. Res. Commun.* **2006**, *344*, 688.
- [51] Desideri, N.; Bolasco, A.; Fioravanti, R.; Monaco, L. P.; Orallo, F.; Yanez, M.; Ortuso, F.; Alcaro, S. *J. Med. Chem.* **2011**, *54*, 2155.
- [52] Tzvetkov, N. T.; Hinz, S.; Küppers, P.; Gastreich, M.; Müller, C. E. *J. Med. Chem.* **2014**, *57*, 6679.
- [53] Legoabe, L. J.; Petzer, A.; Petzer, J. P. *Bioorg. Chem.* **2010**, *45*, 1.
- [54] Cheung, J.; Rudolph, M. J.; Burshteyn, F.; Cassidy, M. S.; Gary, E. N.; Love, J.;

Franklin, M. C.; Height, J. J. *J. Med. Chem.* **2012**, *55*, 10282.

[55] Binda, C.; Wang, J.; Pisani, L.; Caccia, C.; Carotti, A.; Salvati, P.; Edmondson, D. E.; Mattevi, A. *J. Med. Chem.* **2007**, *50*, 5848.

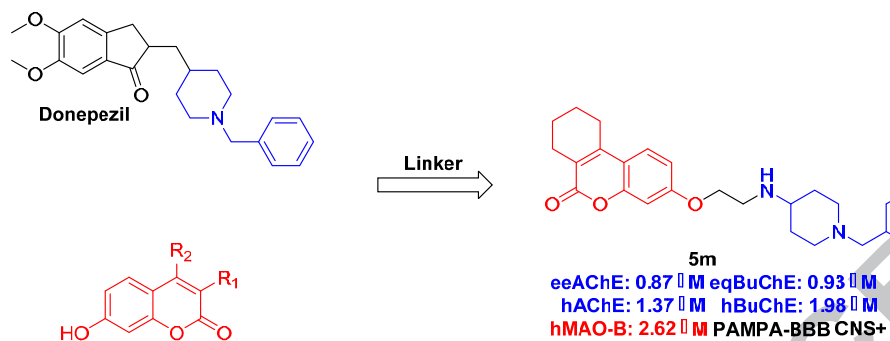
[56] Di, L.; Kerns, E. H.; Fan, K.; McConnell, O. J.; Carter, G. T. *Eur. J. Med. Chem.* **2003**, *38*, 223.

[57] Li, S. Y.; Wang, X. B.; Kong, L. Y. *Eur. J. Med. Chem.* **2014**, *71*, 36.

[58] Zhao, Y. R.; Qu, W.; Liu, W. Y.; Hong, H.; Feng, F.; Chen, H.; Xie, N. *Chin. J. Nat. Med.* **2015**, *13*, 438.

[59] Nepovimova, E.; Uliassi, E.; Korabecny, J.; Peña-Altamira, L. E.; Samez, S.; Pesaresi, A.; Garcia, G. E.; Bartolini, M.; Andrisano, V.; Bergamini, C.; Fato, R.; Lamba, D.; Roberti, M.; Kuca, K.; Monti, B.; Bolognesi, M. L. *J. Med. Chem.* **2014**, *57*, 8576.

## Graphical Abstract



ACCEPTED MANUSCRIPT